PFC/JA-90-33

The Connected Presheath: One-dimensional Models of Neighbouring Objects in Magnetized Plasmas

I.H. Hutchinson

Plasma Fusion Center
Massachusetts Institute of Technology
Cambridge, MA 02139

September, 1990

Submitted to Physics of Fluids B.

This work was supported by the U. S. Department of Energy Contract No. DE-AC02-78ET51013. Reproduction, translation, publication, use and disposal, in whole or in part by or for the United States government is permitted.

The Connected Presheath:

One-dimensional Models of Neighbouring Objects in Magnetized Plasmas.

I.H.Hutchinson

Plasma Fusion Center,

Massachusetts Institute of Technology,

Cambridge, Massachusetts, U.S.A.

Abstract

One-dimensional calculations are presented of plasma flow to multiple objects larger than the ion Larmor radius, when their ion collection presheaths overlap. Situations modelled include the effects of one Langmuir probe on another probe lying on the same field line, and Langmuir probes operated close to a limiter or divertor plate in the edges of magnetic confinement experiments. The results allow quantitative analysis of the operation of Langmuir probes and especially Mach probes for velocity measurements, even when they are close to other structures. New analytic results for inviscid plasmas, and numerical results incorporating shear viscosity are presented. They show that Mach probe measurements in inviscid plasmas experience strong perturbation by connection effects especially for Mach numbers greater than about 0.5. Viscous plasmas are relatively more weakly perturbed, although some distortions occur, especially for large probes. Taking into account these distortions, the viscous model is found to be able to fit recent experimental results.

[PACS numbers: 52.40Hf, 52.70Ds]

I Introduction

When objects with transverse dimensions larger than the ion Larmor radius (ρ_i) are introduced into a plasma, their ion collection is governed by highly anisotropic processes. Ions flow freely along the field but can cross the field only by drift or diffusive effects. Consequently, the presheath, that is the quasineutral region of plasma perturbation due to the probe or object, becomes highly elongated along the field. Ions are accelerated, by potential gradients, up to the sound speed in the parallel direction at the sheath edge; meanwhile the presheath is replenished by cross-field diffusion from the outside plasma. The presheath elongates along the field until cross-field transport becomes sufficient to balance the sonic collection flow, as illustrated in Fig.1.

These processes govern not only the behaviour of the scrape-off layer of tokamaks[1] but also the performance of the diagnostics most widely used to measure the scrape-off plasma: electric (Langmuir) probes of various types[2]. Therefore a detailed understanding of the presheath physics is extremely important. Models that have previously been applied to understanding probe behaviour have focussed primarily on "free" presheaths, i.e. ones that do not extend all the way to the nearest solid object along the field but decay away under the influence of diffusion. There are, however, many practical situations which violate this assumption and in which the presheath connects with some other probe or object along the field. For example, in a hydrogen plasma with electron and ion temperatures, $T_e = T_i = 10$ eV, magnetic field B = 4 T, and transverse diffusivity $D = T_e/16eB$ (the Bohm value), a probe of radius a = 0.002m gives rise to a (free) presheath length of order $L_p = c_s a^2/D = 2m$ (c_s is the sound speed). Often measurements[3] are made much

closer to limiters than this 2 m distance, and indeed, specific experimental studies of the effects of close disturber probes have been carried out[4].

Free presheath models have been studied in some detail. If shear viscosity is ignored, Stangeby[5] has shown that one-dimensional fluid models can be solved analytically even when there is parallel flow in the external plasma. In addition Stangeby has applied kinetic one-dimensional sheath calculations governed by particle sources[6] to probe interpretation[7]. More recent work by Hutchinson[8,9] has shown, however, that shear viscosity is an extremely important effect that is missing from these models. Its inclusion at a level giving momentum diffusivity equal to particle diffusivity decreases the ion collection current by about 30% in a stationary plasma. This may be enough to account for some persistent underestimation of edge plasma densities by Langmuir probes[10]. More importantly, perhaps, this viscosity increases the upstream to downstream current ratio from a Mach probe[11] by up to about a factor of 4. In comparisons of one- and two-dimensional fluid calculations[9] and one-dimensional kinetic models[12] Hutchinson and Chung have shown that shear viscosity is a far more important effect than the difference between these various models[13]. Since a priori theoretical justification of the exact shear viscosity is difficult for the turbulent processes we anticipate to govern edge transport, attempts have been made to resolve the question by experiments[14,15]. However, these experiments often involve measurements relatively close to some kind of plasma "dump" and in some cases the presheaths do connect to the dump. Therefore questions arise as to whether they are a fair evaluation of theories that are worked out for free presheaths.

Models of the scrape-off layer per se generally are compelled to deal with connection effects, because the transverse dimension (scrape-off

length) is itself determined by the flow to the limiters (or divertors). Considerable effort has been devoted to multidimensional modelling of the presheath using substantial computer codes[16]. These codes have the obvious advantage of being able to incorporate the many complex effects such as magnetic field variation, recycling and atomic physics, and complicated geometry. However, the codes are sufficiently complex and the number of adjustable parameters so large that it is often difficult to sort out the competing effects. There is therefore still interest in simplified models of the scrape-off layer, particularly for the physical insight that they provide. They have recently been reviewed by Stangeby and McCracken[1] and a detailed study of self-similar models has been presented by Günther[17].

The purpose of the present work is to study connected presheaths using one-dimensional fluid models with or without shear viscosity.

II Formulation

We suppose that the ions can be adequately described by fluid equations as follows:

$$\nabla_{\parallel}(n_i v_{\parallel}) = -\nabla_{\perp}.(n_i \underline{v}_{\perp}) = S \ , \tag{1}$$

$$\nabla_{\parallel}(n_i m_i v_{\parallel} v_{\parallel}) + (ZT_e + \gamma T_i)\nabla_{\parallel} n_i = -\nabla_{\perp}.(n_i m_i \underline{v}_{\perp} v_{\parallel}) + \nabla_{\perp}.(\eta \nabla_{\perp} v_{\parallel}) = S_m \ , \tag{2}$$

$$n_i \underline{v}_{\perp} = -D\nabla_{\perp} n_i \ , \tag{3}$$

where n_i is the ion density, $\underline{v}$ is the ion velocity, m_i the ion mass, Z the ion charge, η the shear viscosity, and D the cross-field diffusivity. We are here adopting essentially isothermal electrons, and the ion temperature will be taken constant, except that the factor γ allows the sound speed to be taken to correspond to locally adiabatic ion behaviour if desired, so that we define $c_s = [(ZT_e+\gamma T_i)/m_i]^{1/2}$. Calculations by Laux et al.[18], using a full ion energy equation, have shown that the errors involved in this isothermal ion approach are small.

The fluid approach as a whole may be justified first by the observation that for the typical example mentioned in the previous section, if the density is taken as $n_i = 10^{19}$ m^{-3}, and Z = 1, the ion-ion collision mean-free-path is only about 8 cm. Therefore the presheath is quite collisional under these conditions. Second, even if the presheath were not collisional, rather close agreement has been demonstrated between a completely collisionless kinetic model of free presheaths and this fluid model[12]. Thus ion-ion collisions (or the lack of them) constitute a minor effect. This kinetic comparison also justifies the omission of parallel viscosity from equation (2). Ion-electron collisions, if they were appreciable, would represent an important momentum source that is omitted. However, for our

example the ion-electron collision mean-free-path is about 100m, which is longer than most relevant presheaths. Thus we are justified, in most tokamak cases in ignoring ion-electron collisions.

The essence of the one-dimensional approximation is to regard the perpendicular divergences as sources, S and S_m, in essentially one-dimensional (parallel) equations, as illustrated by Fig. 1. For the particle (continuity) source, Stangeby[1,5,13] has used on different occasions S = const. and S $\propto$ n. Neither of these convincingly represents an approximation to the transverse diffusion term. Hutchinson[8,9] has used a more physically reasonable and systematic approximation of the transverse derivatives that leads straightforwardly to

$$S = \frac{D}{a^2} (n_o - n) , \tag{4}$$

where n_o is the density in the outer plasma, n that in the presheath, and a is the transverse dimension of the presheath ($\nabla_\perp \rightarrow 1/a$). For the purposes of calculating the flow to the probe in a *free* presheath, the spatial form of S is not important because it determines only the longitudinal profile of the presheath. However, in calculating connection effects the presheath spatial extent is integral to the problem; therefore in the present context this source choice is important.

The ratio of the momentum source, S_m, to S is important whether or not connection occurs. Systematically approximating Eq.(2), using Eqs.(1) and (3) leads to

$$\begin{aligned} S_m &= m_i v S + \frac{\eta}{a^2} (v_o - v) \\ &= m_i v \nabla_{\|}(n v) + \frac{D}{a^2} (n_o - n + \frac{\eta}{m_i D}) m_i (v_o - v) , \end{aligned} \tag{5}$$

where v refers to the parallel velocity inside the presheath (we drop the ||

suffix) and v_o that outside the presheath. We have here ignored spatial dependence of η. The inviscid case, $\eta = 0$, has $S_m = m_i v S$. More generally, it is appropriate to take $\eta/nm_iD = \alpha$ to represent the ratio of the momentum to particle diffusivity. Hutchinson[19] has advocated a value $\alpha \sim 1$, but the dependence of the results on α is of considerable interest.

The equations are then rendered into normalized form by expressing the velocity as a Mach number, $M = v/c_s$, to obtain:

$$M \frac{dn}{dz} + n \frac{dM}{dz} = \frac{1}{L_p} (n_o - n) \quad , \tag{6}$$

$$\frac{dn}{dz} + n M \frac{dM}{dz} = \frac{1}{L_p} (M_o - M) (n_o - n[1 - \alpha]) \quad , \tag{7}$$

where z is the parallel coordinate and again $L_p = c_s a^2/D$ is the characteristic length of the presheath. These are the equations that have previously been studied[9] for free presheaths. The boundary conditions are that $|M| = 1$ at the sheath edges.

III Uniform External Plasmas

If n_o and M_o are independent of z, then z can be eliminated and the equations solved for n as a function of M by rearranging Eqs. (6) and (7) as

$$L_p \frac{dn}{dz} = \frac{(n_o - n)M - (M_o - M)(n_o - n[1-\alpha])}{M^2 - 1} , \tag{8}$$

$$L_p \frac{dM}{dz} = \frac{(M_o - M)(n_o - n[1-\alpha])M - (n_o - n)}{n(M^2 - 1)} , \tag{9}$$

and dividing to get

$$\frac{dn}{dM} = n \frac{(n_o - n)M - (M_o - M)(n_o - n[1-\alpha])}{(M_o - M)(n_o - n[1-\alpha])M - (n_o - n)} . \tag{10}$$

For a free presheath, the point at infinity (if $\alpha \neq 0$) corresponds to $M = M_o$ and $n = n_o$ and the equation for n(M) is integrated from there to $M = 1$, corresponding to the sheath edge. Subsequently the spatial dependence can be obtained by integrating Eq. (9) to get z(M) and hence implicitly M(z) and n(z). Previous calculations have placed little emphasis on the spatial variation since it does not affect the collection flux, for a free presheath. For a connected presheath, however, the spatial form is vital. Even so, a similar approach can be adopted as follows.

Consider a connected presheath, bounded at both ends by a probe and hence with outflow boundary condition $|M| = 1$. Clearly if the distance between the two probes, L_c say, is smaller than the characteristic length $c_s a^2/D$, then the density inside the presheath will everywhere be less than n_o (the outside density) because as the connection length gets smaller there is less and less length available to supply the cross-field flux which balances the sonic outflow. Fig. 2 illustrates the situation. The mach number ranges from -1 to +1 in the presheath because of the boundary

conditions. Therefore there is still a point in the presheath at which $M = M_o$. Call this point z_m and the density there n_m. If we know the value of n_m, we can still solve the presheath equation by integrating Eq (10) from $M = M_o$ to 1 and from $M = -M_o$ to 1, obtaining n(M) for two halves of the presheath. Then the spatial dependence can be obtained as before by integrating Eq. (9) to get z(M) for these two halves and fitting them together at z_m. This has been done numerically using a straightforward generalization of the code used previously[9]. Fig 3. shows the results of this process for a specific choice of n_m and α and a range of M_o.

Thus we can solve the connected presheath problem for uniform M_o and n_o implicitly in essentially the same way as for a free presheath, using simple quadrature. We cannot specify L_c a priori, but must specify n_m. However, by studying the whole range of n_m we cover the whole range of L_c. Results are shown in Fig 4. It should be noted that the numerical scheme experiences some difficulties with integrations exceeding a dimensionless distance of about 10, which is why the results of Fig. 4 extend no further. This is because of the proximity to singularities in the equations which magnifies small numerical errors.

Inspection of Fig. 4 indicates the perhaps somewhat surprising result that the sheath-edge density (and hence the probe flux) is less affected by a limited connection length when the external flow velocity is away from the probe than it is when the velocity is towards the probe. This appears to be because the most important effect of the connection is to impose the condition $|M| = 1$ at the boundary. If the external flow is already substantially away from the probe, requiring it to flow away at the sound speed is not such a big perturbation as it is if the distant flow is toward the probe in the free case.

In addition to these numerical results, a closed form analytic solution for the $\alpha = 0$ case has been obtained. This capitalizes on the well known fact that the inviscid equations have the solution:

$$n = \frac{n_m}{1 + M^2 - M_o M} \quad , \tag{11}$$

independent of the spatial form of S. The integration to obtain z(M) has previously[5] been performed for the cases S = const. and $S \propto n$. It can also be done for the present, more physical, case $S \propto (n_o - n)$, with n_o constant. Substituting the solution (11) into Eq. (9) (with $\alpha = 0$) and integrating we obtain

$$-\int \frac{dz}{L_p} = \frac{n_m}{n_o} \int \frac{M^2 - 1}{(M^2 - M_o M + N)(M^2 - M_o M + 1)} dM \quad , \tag{12}$$

where $N = (n_o - n_m)/n_o$. The integration may be done by partial fractions. Putting $M = 1$ at $z = 0$ (so that we are treating a presheath on the negative z side) we get after some algbra:

$$\begin{aligned} -\frac{z}{L_p} = &-\frac{2N+2-M_o^2}{\sqrt{(4N-M_o^2)}} \left[\arctan\left\{ \frac{2M - M_o}{\sqrt{(4N-M_o^2)}} \right\} - \arctan\left\{ \frac{2 - M_o}{\sqrt{(4N-M_o^2)}} \right\} \right] \\ &+ \frac{4 - M_o^2}{\sqrt{(4-M_o^2)}} \left[\arctan\left\{ \frac{2M - M_o}{\sqrt{(4-M_o^2)}} \right\} - \arctan\left\{ \frac{2 - M_o}{\sqrt{(4-M_o^2)}} \right\} \right] \\ &+ \frac{M_o}{2} \ln \left| \frac{2 - M_o}{M^2 - M_o M + 1} \; \frac{M^2 - M_o M + N}{1 + N - M_o} \right| \quad . \end{aligned} \tag{13}$$

This general expression yields useful simplifications in various limits which we list here for convenience.

In the limit $N \to 0$ corresponding to a free presheath ($n_m = n_o$)

$$-\frac{z}{L_p} = \sqrt{(2-M_o^2)}\left[\arctan\left\{\frac{2M - M_o}{\sqrt{(4-M_o^2)}}\right\} - \arctan\left\{\frac{2 - M_o}{\sqrt{(4-M_o^2)}}\right\}\right]$$

$$+\frac{1}{M_o}\ln|M| + \left(M_o - \frac{1}{M_o}\right)\ln\left|\frac{M-M_o}{1-M_o}\right| - \frac{M_o}{2}\ln\left|\frac{M^2-M_oM+1}{2 - M_o}\right| \quad . \tag{14}$$

In the limit $M_o \to 0$, corresponding to stationary external plasma

$$-\frac{z}{L_p} = -\frac{1+N}{\sqrt{N}}\left[\arctan\left\{\frac{M}{\sqrt{N}}\right\} - \arctan\left\{\frac{1}{\sqrt{N}}\right\}\right] + 2\left[\arctan(M) - \frac{\pi}{4}\right] \quad . \tag{15}$$

And in the limit where both N and $M_o \to 0$

$$-\frac{z}{L_p} = \frac{1}{M} - 1 + 2\left[\arctan(M) - \frac{\pi}{4}\right] \quad . \tag{16}$$

This last expression illustrates one of the problematical features of the inviscid free presheath, in that asymptotically $M \sim 1/|z|$, while $n_o - n \sim 1/z^2$ at large distances. Thus the M perturbation has a greater extent than the n perturbation. This is even worse for negative M_o, where Eq. (14) shows that M never changes sign and therefore never reaches M_o, a fact that has been discussed before[9].

IV Nonuniform External Plasmas

The solutions developed in the previous section are relevant to cases where the external plasma parameters are independent of the parallel component, z. As such they may reasonably be taken to model, for example, the presheath between two adjacent probes of the same size, or a simple scrape-off layer itself (in so far as a one-dimensional treatment of this is appropriate). However, if we are interested, for example in the behaviour of the presheath of a probe close to a larger perturbing object, limiter, disturber or whatever, then that presheath does not see a uniform external plasma. Instead it sees as its external plasma the *internal* plasma of the larger object (we hereafter call the larger object the "dump", for brevity). Fig. 5 illustrates the physical situation. Naturally, the dump plasma has variation over a longitudinal distance of order its characteristic length $L_d = c_s d^2/D$, where d is the effective transverse dimension of the dump's presheath. Although this will be longer than the probe's presheath, L_p, (since d > a by presumption) there may nevertheless be substantial plasma variation over a distance L_p especially if the probe is close to the dump. Therefore we are interested in modelling presheaths for which the external parameters, n_o and M_o, are functions of z.

For such situations the equations cannot be integrated for n(M) in the manner of the previous section. Instead we must solve the equations in z-space with boundary conditions and $n_o(z)$ and $M_o(z)$ specified.

A one-dimensional code has been written to obtain this solution. The code uses the numerical methods described by Patankar[20]. The momentum equation is expressed in convection-diffusion form and advanced by a hybrid difference scheme. (A parallel viscosity term is included but in the present

work the coefficient is set to a negligible value so that the scheme is essentially an upwind difference scheme). The continuity equation is advanced by a pressure correction scheme accounting for compressibility. This scheme is thus essentially similar to that employed in the much more sophisticated code of Braams[16]. A nonuniform mesh is employed on the domain $0 \le z \le 1$, setting $z_i = 3u_i^2 - 2u_i^3$ and $u_i = i/i_{max}$ for $i = 0, 1, \ldots i_{max}$. This then gives optimum resolution of the slope singularity at the boundaries (subscript s : sheath-edge), where it can be shown that $(n - n_s) \sim \sqrt{|z - z_s|}$.

The time-dependent equations are iterated to convergence, which then represents the steady state solution. However, a problem arises because the upwind difference scheme is only 1st order accurate[21]. It is found that for the specific case $\alpha = 1$, $M_o = 0$, and $L_p = 0.1$, which separates the two boundaries sufficiently that the presheaths are free and so the flux is known from previous work (viz $n_s/n_o = 0.352$), the code obtains an edge flux larger by $1/i_{max}$. Thus for 101 mesh points there is an error of about 3%. Although this is not too severe a problem for the mesh of size 101 used in the present work, it would be a substantial error for a mesh any smaller. A simple expedient has been found to provide (apparently) second order spatial accuracy while retaining the stability benefits of the hybrid scheme. The equations are iterated to convergence, but then the residual error in the momentum equation is calculated using *central* differences. This residual is added to the momentum equation as a (fixed) correction source and the equation iterated to convergence again. Since the first stage need not be pursued to a high degree of convergence, this two-step process takes little additional computing time.

Comparisons have also been carried out between the code results for $\alpha =$

0 and the analytic results of the previous section. These show negligible discrepancies; although some care must be exercised to avoid density errors in the distant presheath in cases with very small L_p, because of the difference in velocity and density perturbation distance mentioned in the previous section. The discrepancy in the collected flux is negligible even if such errors are not avoided.

This code can, of course, reproduce the results for cases where the external plasma is uniform, and do so with *specified* L_p. Fig. 2 was in fact obtained with this code. However, a perhaps more interesting problem to study is when the external parameters vary with z. To be specific, the problem chosen for study here is the behaviour of a probe in the presheath of a larger dump. The dump plasma is supposed to obey the same equations, with the same transport coefficients, and itself to reside in a wider plasma of density n_∞ uniform, and $M_\infty = 0$. Thus, the spatial variation of the dump plasma is just a solution of a uniform external plasma problem, but with a different transverse dimension, d. This plasma then constitutes the external plasma for the solution of the probe's presheath. For present purposes we take the dump to possess a free presheath. Therefore the spatial variation of the dump plasma is determined by the value of the viscosity, α, and the characteristic length, $L_d = c_s a^2/D$.

It is helpful to have an explicit parametric form of the dump plasma profile, and therefore an analytic fit has been obtained to the results of numerical calculations. Expressions of the following form are fitted to the calculated dump presheath

$$n(x) = n_\infty \left[1 - \exp(a_n + b_n\sqrt{|x|} + c_n|x|) \right] \quad , \tag{17}$$

$$M(x) = - \frac{x}{|x|} \exp(b_v\sqrt{|x|} + c_v|x|) \quad , \tag{18}$$

where x is the normalized distance, z/L_d, The fits are extremely good,

giving, for example, less than 4% error (< 0.025 absolute error) over $3\frac{1}{2}$ decades in v for $\alpha = 1$, and even better accuracy for $(n_\infty - n)$. The coefficients for $\alpha = 1$ and 0 are given in table 1. For intermediate values of α an interpolation of the coefficients linear in $\sqrt{\alpha}$ is used between these sets, and gives reasonable fits.

In order to calculate the behaviour of a probe in a plasma of this form, two runs of the presheath code are used, for each position. The first models the presheath connecting the probe to the dump: the downstream side of the probe (since the velocity in the dump plasma is towards the dump). This is the connected presheath, whose length is fixed as the separation between the probe and the dump. The second run models the upstream side of the probe, where the presheath is free. In this case the length modelled is taken to be long enough that the boundary condition at the end of the computational domain does not affect the near solution. The external plasma variation is taken, in both cases, to be given by the appropriate form of Eqs. (17) and (18) as illustrated in Fig. 6.

The key quantity of interest for probe behaviour is then the flux into the sheath, which is equal to the sound speed times the edge density. Results are given in tables 2 and 3 and plotted in Figs. 7 and 8 for the edge density normalized to n_∞, and the ratio of the upstream to downstream fluxes. These are given as a function of the dimensionless distance, x, between the probe and the dump in units of the dump presheath characteristic length (z/L_d) and the velocity and density ($M_o(x)$ and $n_o(x)$) at the probe position are noted. Three representative cases are calculated for the ratio of the probe characteristic presheath length to the dump characteristic length:

$$L = \frac{L_p}{L_d} = \frac{a^2}{d^2} \quad . \tag{19}$$

The largest value of L corresponds to a = 0.45 d (L = .02), a probe about half the transverse size of the dump. The smallest represents a probe one tenth of the size of the dump.

A remarkable observation is that the upstream flux observed is almost completely independent of both L and the distance x. A partial understanding of this fact may be obtained by considering the small and large x limits. As $x \to 0$ the probe becomes part of the dump and so its upstream collection should be just that of the dump, i.e. that of any probe in a plasma characterized by n_∞ and M_∞. On the other hand, as $x \to \infty$ the probe is unaffected by the dump, and so again it just collects from the external plasma, n_∞, M_∞. That intermediate values of x should give also the same value is not obvious a priori, but is observed in the calculations. Actually the x = 0 upstream collection is *not* exactly equal to the free presheath value in the calculations, even though physically it should be. This is because our model separates the probe and dump presheaths and does not account for the fact that the probe presheath becomes part of the dump presheath and therefore ought to participate in the transverse sources that determine the dump presheath. That the discrepancy is only ~ 10% for $\alpha = 0$ and even less for $\alpha = 1$ indicates roughly the error involved in these one-dimensional approximations. Differences in upstream collection between the different L cases are so small (< 1% typically) that we tabulate the upstream flux only for the L = 0.2 case.

The downstream flux is, of course, a strong function of x. It decreases as x decreases because (i) n_o is decreasing (ii) M_o is increasing and (iii) connection to the dump is increasing. From the diagnostic viewpoint, (i) and

(ii) are the factors that a probe would like to measure, in order to establish the plasma density and flow pattern near the dump, for example. The connection effects constitute a perturbation of the measurement from what would be obtained if the probe presheath were free. For the $\alpha = 1$ case, inspection of Fig. 7 indicates that the downstream current density to a probe with presheath length L (in units of the dump's presheath) at a point x is very roughly equal to what would have been observed with an infinitesimal probe ($L = 0$) at a point closer to the dump by a distance L, i.e. at $x - L$. This algorithm obviously breaks down for distances closer than L, but it gives a plausible physical summary of the connection effects. A similar summary can be formulated for the $\alpha = 0$ case, except that the shift corresponds to about 3L, presumably because the effective length of the presheaths (both dump and probe) are longer (for M) in units of L_d.

The flow measurement, using the ratio of upstream to downstream probe currents is most affected by the connection. The importance of the connection for Mach probe interpretation is shown in Fig 8. where the ratios are plotted against velocity (M_o), together with the theoretical ratio for a free presheath at the same velocity. (For the $\alpha = 1$ case we use the expression $R = \exp(M/M_c)$ for the free ratio, with $M_c = 0.41$ [9]. For the $\alpha = 0$ case the analytic result $R = (2+M)/(2-M)$ is used). These show, for example, that if $\alpha = 1$ the use of the free presheath curve for interpretation of Mach probe data gives negligible error up to almost $M = 1$ when using very small probes ($L = 0.01$); for larger probes, an error of less than 20% in M will occur up to about $M = 0.7$ for $L = 0.05$, but for $L = 0.2$ the error is about 30% up to about $M = 0.4$ and rapidly increasing above that. On the other hand, if $\alpha = 0$, even a very small probe ($L=0.01$) experiences greater than 20% error above $M = 0.5$ and progressively worse for larger probes.

V Experimental Comparison

Recent experiments by Chung et al[14] investigated the behaviour of a probe in the flow pattern of a dump. The intention of the experiments was to try to establish what is the best value of α in typical Mach probe experiments by a comparison of the results with theory. Since independent velocity measurements were not available, the authors attempted to obtain self-consistent fits to the data of calculations that modelled both the probe and the dump presheaths with the same theory and α. This process seemed to indicate that a viscid ($\alpha \sim 0.5$) approach was better. However, the fits were relatively poor. This was attributed to the connection problem, which was not modelled, since free-presheath theory was used. It seems that these experiments ought to be closely approximated by the present theory and so we present here a comparison with the experimental results.

In comparing with the experiments, the diffusivity, D, which determines the length scale of the entire problem, is taken as an adjustable parameter, in the same manner as Chung et al. The ratio of probe radius to dump radius in the experiments was 6.5/16, which we will take as reasonably modelled by $L = 0.2$. (Close enough to the nominal value $(6.5/16)^2 = 0.17$). Then we compare the theoretical upstream/downstream ratio with that observed in the experiments, but with the parallel length scale (effectively L_d) as an adjustable parameter. Fig. 9 shows an overlay of the theoretical lines for $\alpha = 1$ and $\alpha = 0$ and the experimental points.

The fit of the $\alpha = 1$ theory is remarkably good, within experimental uncertainty over the whole range. The fit is much better than could be obtained using the free-presheath analysis. On the other hand, the inviscid, $\alpha = 0$ theory cannot fit the data within experimental uncertainty, even with

the connection effects included.

This comparison provides evidence both that the present results are capable of explaining experimental observations and also that viscid ($\alpha \sim 1$) modelling is essential.

It may be noted also that upstream collection current independent of distance from the dump was observed in the experiments, in good agreement with the present results.

VI Discussion

The models of section III, using uniform external parameters, are appropriate for one-dimensional modelling of simple scrape-off layers, although generally the scrape-off layer is considered to adjust its transverse length scale (the scrape-off length) in such a way as to balance the collection flux, whereas we have been speaking as if that length, a, were fixed. An important contribution of the present work to scrape-off layer modelling is to provide solutions that use more physical transverse source both in terms of its n-dependence ($\propto n_o - n$) and in terms of the viscosity.

For probe analysis, on the other hand, section III applies convincingly only to probes of the same size, on the same field line. For independent probes in tokamak edge plasmas perfect alignment would be rare. However, probes with relatively small parallel separation could be constructed with the necessary alignment. One possible advantage that might be useful for such probes, measuring the ends of a strongly connected presheath, is that their collection appears to be less influenced by viscosity. However, it is not completely clear that the one-dimensional model is reliable in this respect.

The calculations of section IV, accounting for the spatial variation of the external plasma, should be useful for interpreting probes in the shadow of limiters or divertors. The appropriate transverse scale length to use for d, is presumably the scrape-off length. Therefore the results should model probes that are smaller than the scrape-off length by factors of roughly 0.45, 0.22, and 0.1. In the last case, viscid plasmas experience only very small perturbations due to connection.

There is perhaps some question whether scrape-off plasmas have spatial forms exactly similar to the dump. Moreover, experiments seem to indicate that under some circumstances the infilling of the downstream presheath is substantially faster than might be expected based on the diffusivity characteristic of the whole scrape-off plasma[3]. However, futher theoretical and experimental work is necessary to determine this.

All the present results must be accompanied by the caveat that the one-dimensional approximation requires verification by two-dimensional calculations. Past comparisons have shown the one-dimensional approximation to work very well. However, it is possible that the agreement would not be so good for connected presheaths as it is for free. In addition, various other important factors are omitted from the present model, such as: magnetic field variation along the presheath, ionization, charge-exchange and other atomic effects, and spatial variation of diffusivity and temperature. These omissions can only be rectified by further, more elaborate modelling, but the present simple model appears to have most of the essential physics to understand the behaviour of the connected presheath.

Acknowledgements

This work was supported by the US Department of Energy under contract DE/AC02-78ET51013.

References

1. P.C.Stangeby and G.M.McCracken, Nucl. Fusion 30, 1225 (1990).
2. I.H.Hutchinson, *Principles of Plasma Diagnostics*, (Cambridge University Press, New York 1987).
3. e.g. J.Allen and P.J.Harbour, J. Nucl. Materials 145-147, 264 (1987).
4. G.F.Matthews, P.C.Stangeby and P.Sewell, J. Nucl. Materials 145-147, 220 (1987).
5. P.C.Stangeby, Phys. Fluids 27, 2699 (1984).
6. G.A.Emmert, R.M.Wieland,A.T.Mense, and J.N.Davidson, Phys. Fluids 23, 803 (1980).
7. P.C.Stangeby, J. Phys. D 15, 1007 (1982).
8. I.H.Hutchinson, Phys. Fluids 30, 3777 (1987).
9. I.H.Hutchinson, Phys. Rev. A 37, 4358 (1988).
10. A.Pospieszczyk, F.Aumayr, H.L.Bay et al. J. Nucl. Materials 162-164, 574 (1989).
11. P.J.Harbour and G.Proudfoot, J. Nucl. Materials 121, 222 (1984).
12. K-S.Chung and I.H.Hutchinson Phys. Rev. A 38, 4721 (1988).
13. c.f. also: R.C.Bissel, P.C.Johnson and P.C.Stangeby, Phys. Fluids B 1, 1133 (1989).
14. K-S.Chung, I.H.Hutchinson, B.LaBombard and R.W.Conn, Phys. Fluids B 1, 2229 (1989).
15. S.L.Gulick ,B.L.Stansfield and C.Boucher, Bull. A.P.S., 34, 2026 (1989).
16. B.J.Braams, NET report No. 68, (Max Planck Institut für Plasmaphysik,

Garching 1987).

17. K.Günther, Contrib. Plasma Phys. 28, 365 (1988).

18. M.Laux, H.Grothe, K.Günther,, A.Herrmann, D.Hildebrandt, P.Pech, H.-D.Reiner and H.Wolff, J. Nucl. Materials 162-164, 200 (1989).

19. I.H.Hutchinson, Phys. Fluids 31, 2728 (1988).

20. S.V.Patankar, *Numerical Heat Transfer and Fluid Flow* (Hemisphere, New York, 1980).

21. R.D.Richtmyer and K.W.Morton *Difference Methods for Initial-Value Problems* (Wiley, New York, 1967).

Tables

α	a_n	b_n	c_n	b_v	c_v
1	-0.434	-1.112	-0.638	-1.810	-0.370
0	-0.690	-1.622	+0.096	-1.091	+0.041

Table 1. Coefficients for the fit of the presheath spatial form, Eqs. (17) and (18), for the viscid, $\alpha = 1$, and inviscid, $\alpha = 0$, cases.

Table 2. Presheath current data for viscid plasmas.

Distance	Velocity	Density	Up	Down	Ratio	Down	Ratio	Down	Ratio	Ratio
				L=0.2		L=0.05		L=0.01		L=0
0.010	0.831	0.424	0.362			0.017	20.692	0.043	8.392	7.596
0.020	0.768	0.453	0.362			0.031	11.648	0.052	6.976	6.516
0.040	0.686	0.494	0.362	0.022	16.558	0.052	6.994	0.067	5.416	5.330
0.060	0.628	0.525	0.362	0.032	11.181	0.064	5.623	0.079	4.602	4.624
0.100	0.544	0.572	0.361	0.052	7.011	0.086	4.220	0.098	3.680	3.766
0.200	0.413	0.653	0.360	0.091	3.943	0.125	2.875	0.136	2.643	2.741
0.400	0.275	0.751	0.358	0.151	2.380	0.181	1.983	0.190	1.887	1.954
0.600	0.197	0.813	0.357	0.194	1.841	0.219	1.626	0.227	1.570	1.617
1.000	0.113	0.887	0.355	0.252	1.409	0.270	1.317	0.276	1.287	1.317
1.500	0.063	0.936	0.354	0.294	1.204	0.305	1.162			1.165
2.000	0.037	0.962	0.354	0.318	1.114	0.325	1.090			1.094
4.000	0.006	0.995	0.353	0.347	1.017					1.015
6.000	0.001	0.999	0.353	0.352	1.002					1.003

Table 3. Presheath current data for inviscid plasmas.

Distance	Velocity	Density	Up	Down	Ratio	Down	Ratio	Down	Ratio	Ratio
				L=0.2		L=0.05		L=0.01		L=0
0.020	0.858	0.538	0.553			0.049	11.332	0.114	4.847	2.502
0.100	0.711	0.584	0.551	0.068	8.143	0.142	3.880	0.197	2.800	2.103
0.200	0.619	0.618	0.549	0.118	4.650	0.197	2.790	0.239	2.302	1.896
0.400	0.510	0.662	0.543	0.186	2.912	0.256	2.120	0.289	1.881	1.684
0.600	0.440	0.694	0.539	0.232	2.325	0.293	1.842	0.322	1.677	1.564
1.000	0.350	0.741	0.533	0.291	1.834	0.339	1.571	0.363	1.470	1.424
1.500	0.279	0.782	0.528	0.337	1.565	0.375	1.405			1.325
2.000	0.232	0.812	0.523	0.368	1.423	0.399	1.311			1.262
4.000	0.133	0.883	0.512	0.429	1.195	0.448	1.143			1.142
6.000	0.088	0.919	0.507	0.455	1.115					1.092
9.000	0.055	0.948	0.502	0.474	1.059					1.056

Figure Captions

Fig 1. Schematic diagram of the physical situation to which the one-dimensional model of the connected presheath corresponds.

Fig 2. Variation of density and Mach number in a connected presheath. (Actual values for this case: $M_o = 0.2$, $L_p = 1$, $\alpha = 1$).

Fig 3. An example of a set of presheath shapes, calculated by integration of the equation for n(M); with $n_m = 0.7$ and a range of values of flow velocity, M_o. (a) n(M) solutions; (b) Mach number, M(z), with M_o ranging from 0 to 0.95 in steps of 0.05; (c) Density for the same M_o range. The distance is dimensionless, normalized to L_p.

Fig 4. Compilation of the results of integrations like those in Fig 3, showing the sheath-edge density (and hence the collection flux) as a function of the total connection length between the two boundaries (in normalized units) for a flow velocity ranging from -0.9 to 0.9 in steps of 0.1. (a) $\alpha = 1$. (b) $\alpha = 0.1$.

Fig 5. Schematic illustration of the presheath configuration of a probe in the neigbourhood of a larger perturbing object (the "dump").

Fig 6. Example of the solution for a probe in the shadow of a dump. (a) The downstream, connected presheath, computed with the domain $0 \leq z \leq 1$ corresponding to $-0.4 \leq x \leq 0$, the distance of the probe from the dump being 0.4 in units of L_d. (b) The corresponding upstream, (effectively) free

presheath, with computational domain $0 \leq z \leq 1$ corresponding to $-8.4 \leq x \leq -0.4$ in units of L_d. In both cases $\alpha = 1$, and $L_p/L_d = L = 0.2$. The external values, M_o and n_o, are shown as dotted lines.

Fig 7. Normalized downstream collection current density and velocity as a function of normalized distance from the dump for three different ratios of probe presheath length to dump presheath length $L = L_p/L_d$. (a) $\alpha = 1$ (b) $\alpha = 0$.

Fig 8. Upstream to downstream current ratio for a Mach probe in the shadow of a dump for different presheath length ratios, L. (a) $\alpha = 1$. (b) $\alpha = 0$.

Fig 9. Fit of the theoretical models to experiment. Points and the shaded area are the data of Chung et al. [ref 14, fig. 11(a)]. Solid line is the $\alpha = 1$ theory, which fits the data well. Dashed line is the $\alpha = 0$ theory (over normalized distance 0 to 6), which cannot be made to fit. Dotted line is the free presheath fit (for $\alpha = 0.5$) of ref 14, which also shows substantial discrepancies.

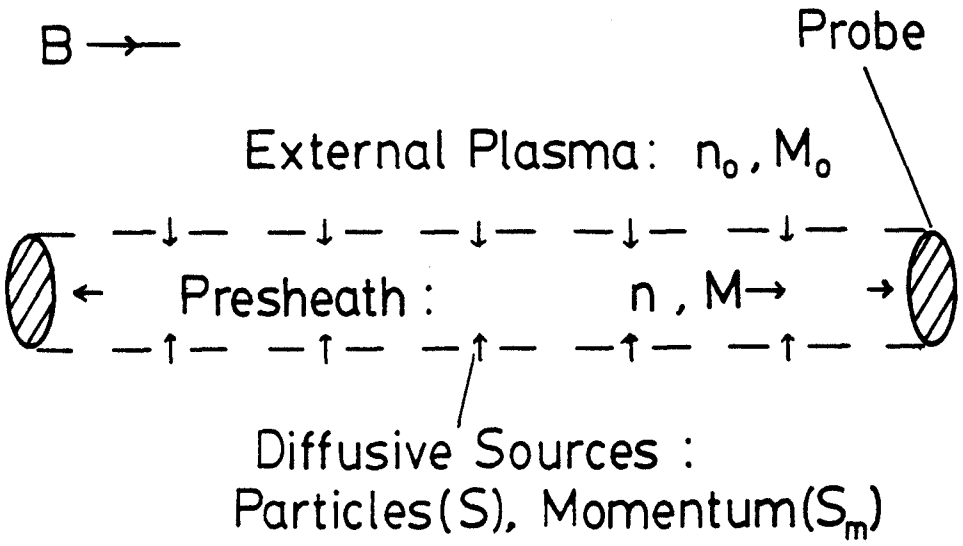
B
Probe
External Plasma: n_o, M_o
Presheath : n , M
Diffusive Sources :
Particles(S), Momentum(S_m)

Fig. 1

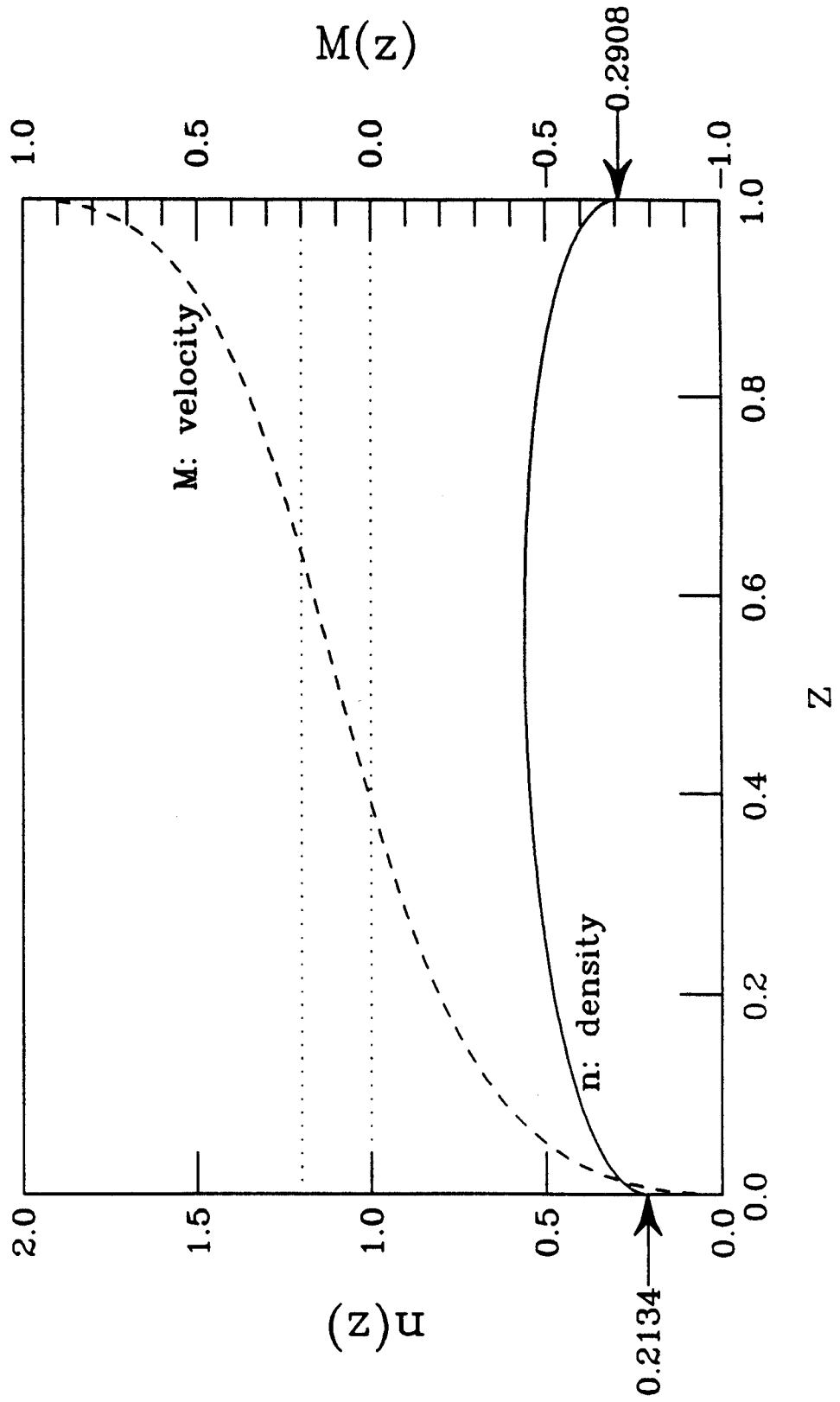
M(z)
n(z)
z
M: velocity
n: density
0.2908
0.2134
1.0
0.5
0.0
-0.5
-1.0
2.0
1.5
1.0
0.5
0.0
0.2
0.4
0.6
0.8

Fig. 2

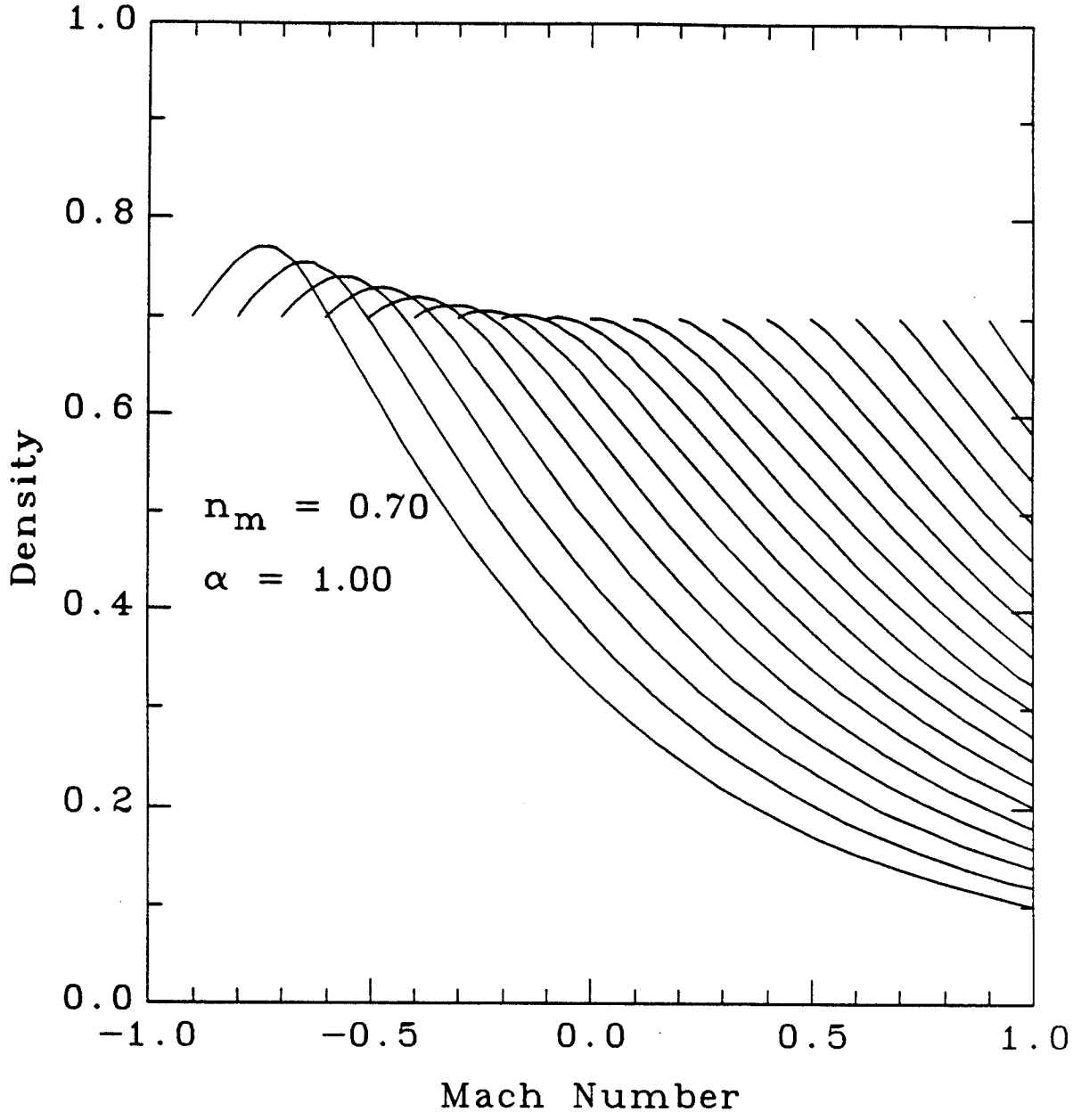

Fig. 3(a)

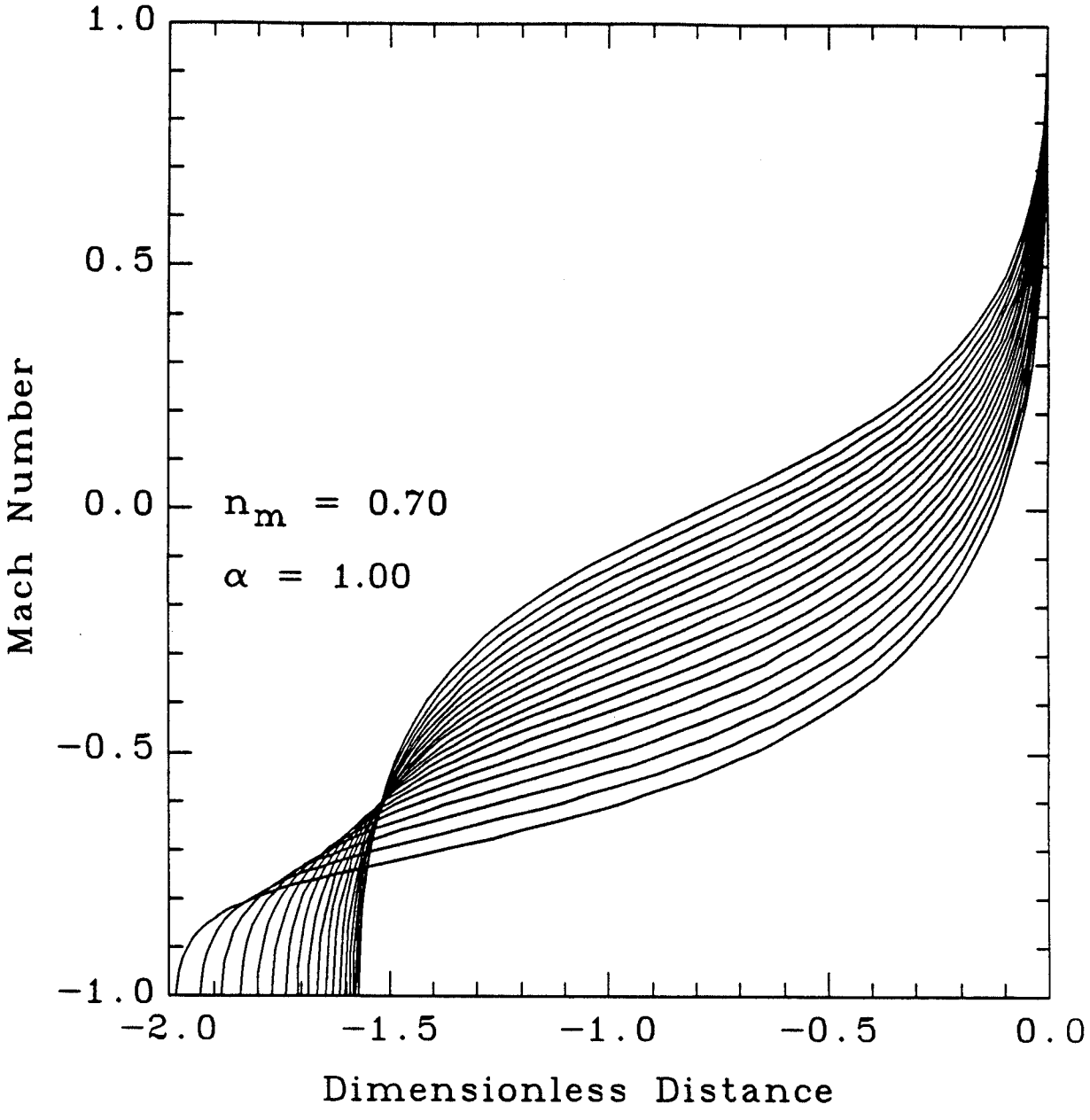
1.0
0.5
0.0
−0.5
−1.0
Mach Number
n_m = 0.70
α = 1.00
−2.0
−1.5
−1.0
−0.5
0.0
Dimensionless Distance

Fig. 3(b)

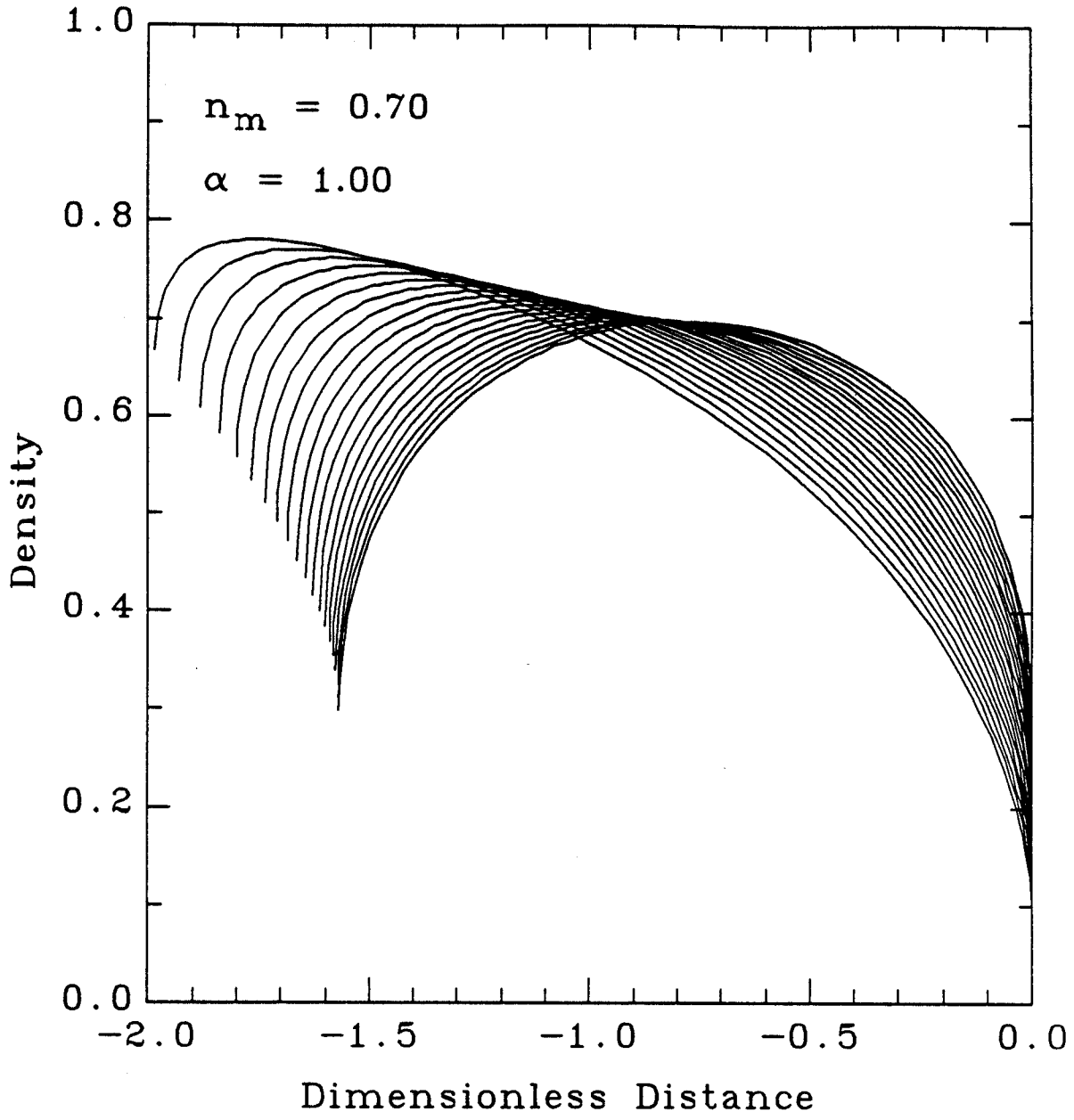
1.0
0.8
0.6
0.4
0.2
0.0
Density
n_m = 0.70
α = 1.00
−2.0
−1.5
−1.0
−0.5
0.0
Dimensionless Distance

Fig. 3(c)

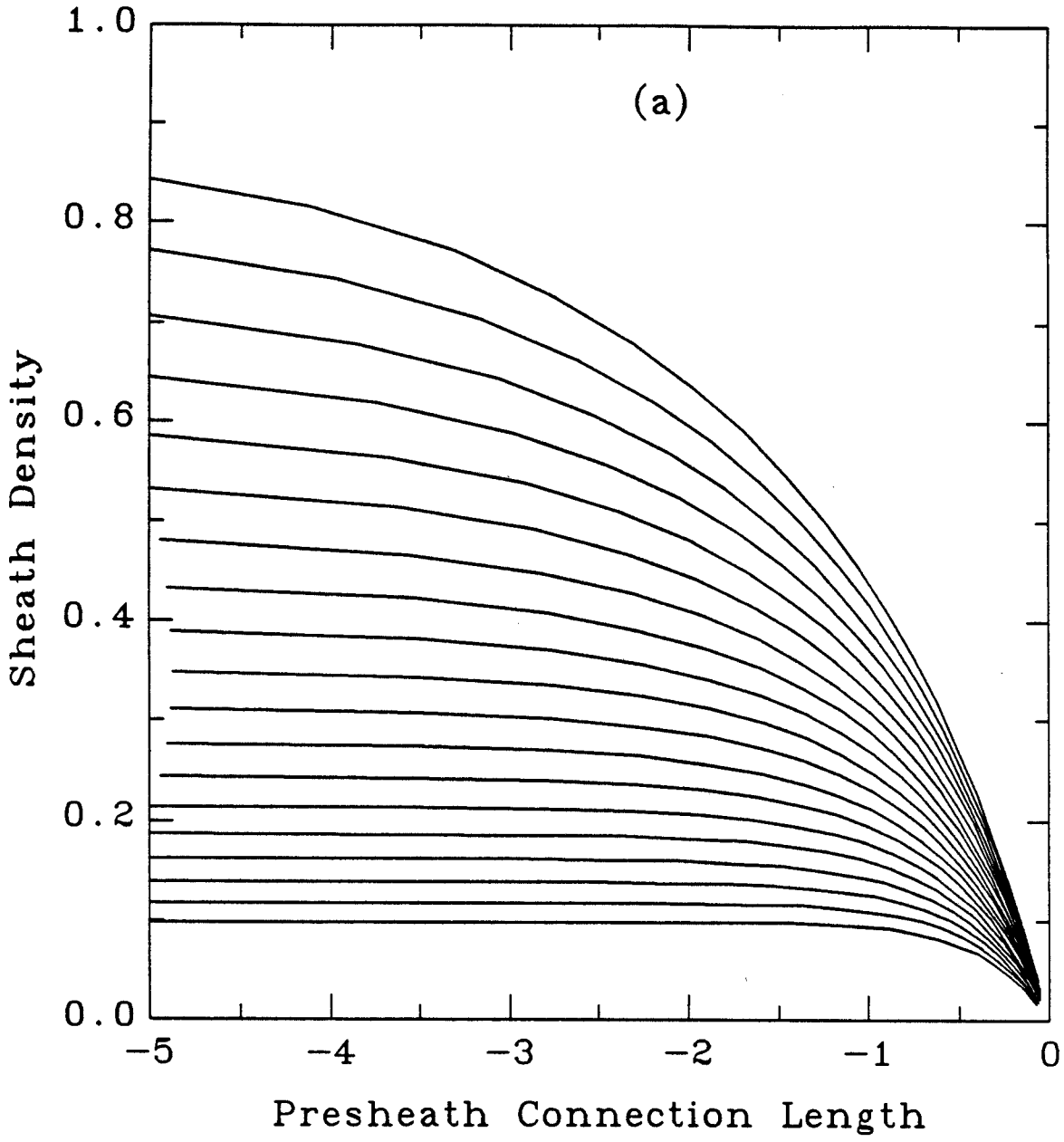
1.0
0.8
0.6
0.4
0.2
0.0
Sheath Density
(a)
−5
−4
−3
−2
−1
0
Presheath Connection Length

Fig. 4(a)

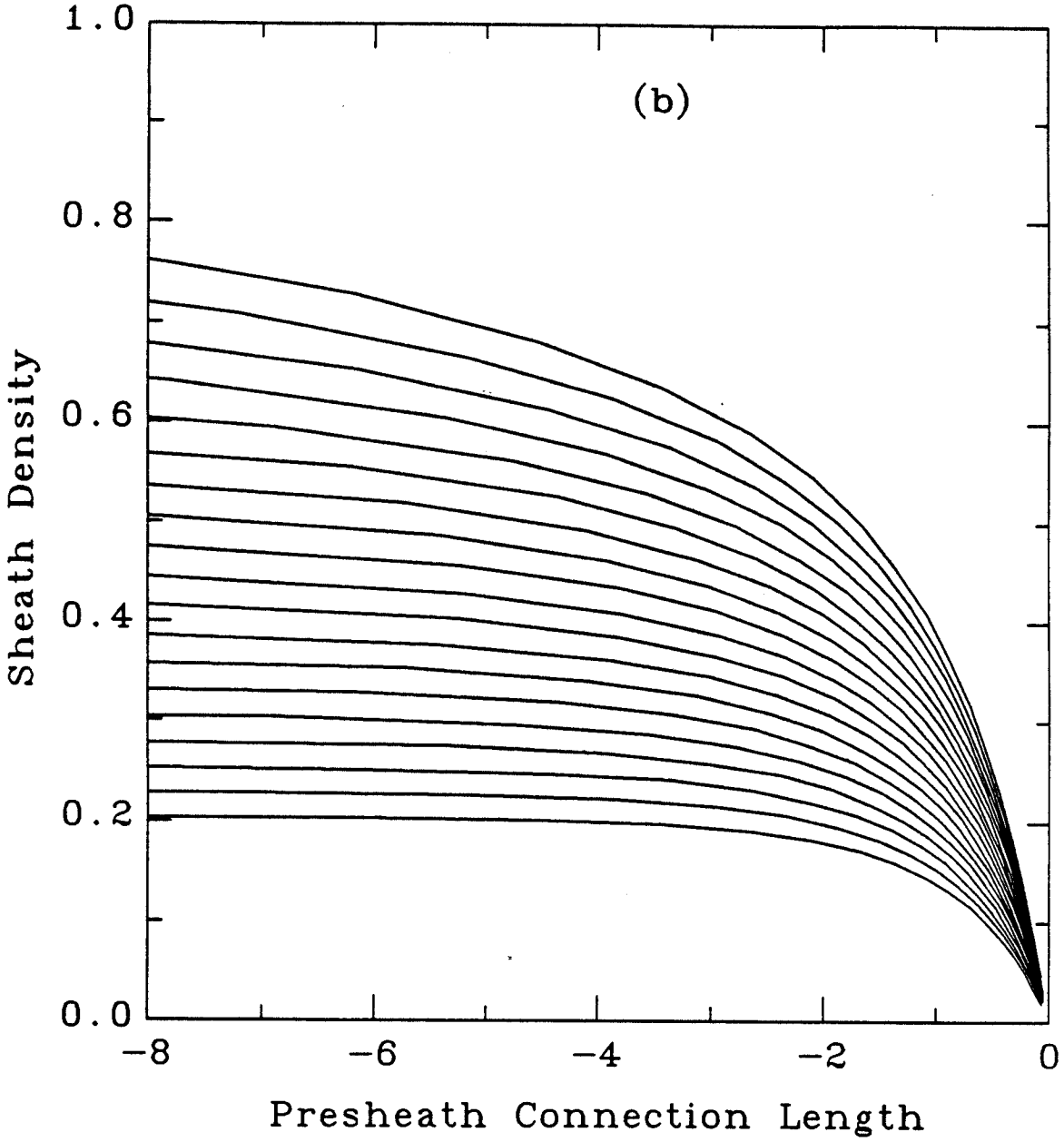
1.0
0.8
0.6
0.4
0.2
0.0
(b)
Sheath Density
−8
−6
−4
−2
0
Presheath Connection Length

Fig. 4(b)

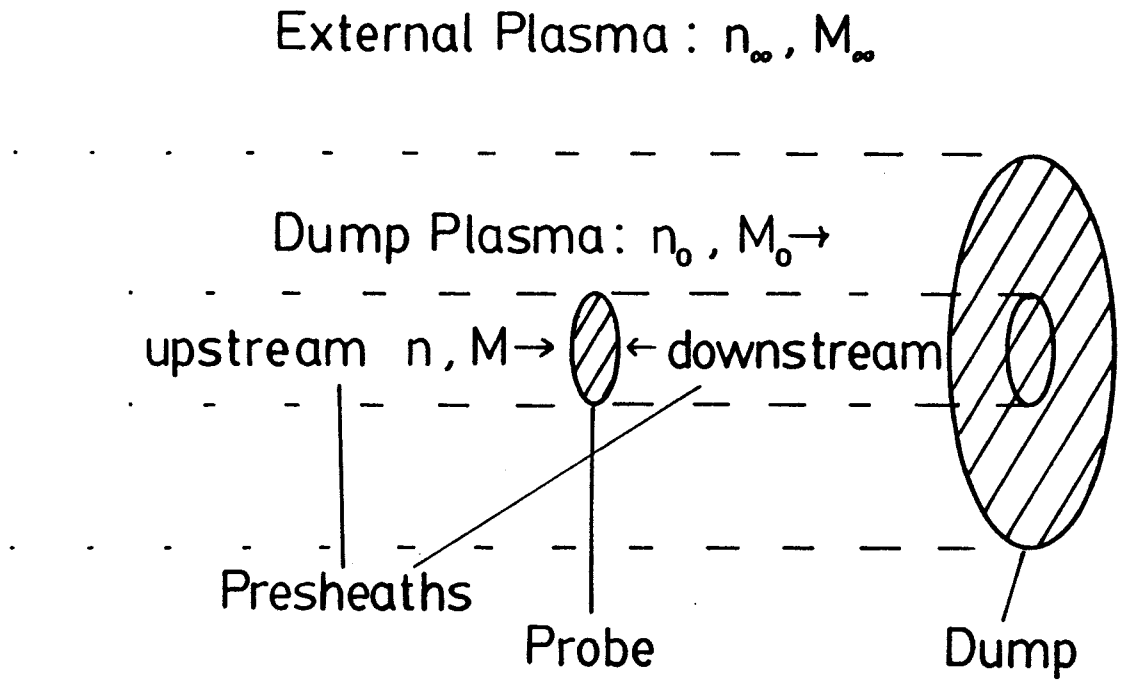
External Plasma : n_∞ , M_∞
Dump Plasma: n_0 , $M_0 \rightarrow$
upstream n , M→
←downstream
Presheaths
Probe
Dump

Fig. 5

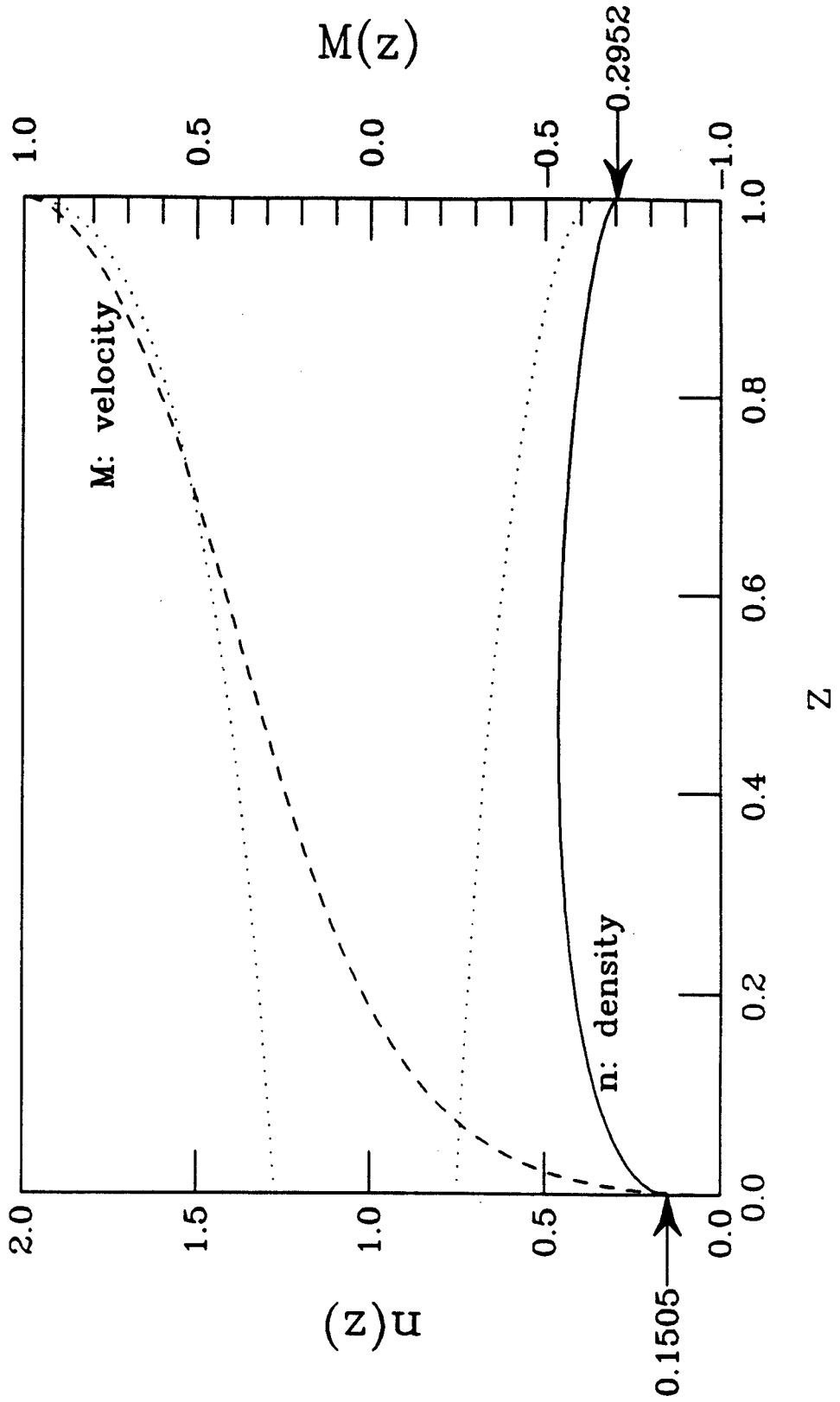
M(z)
n(z)
z
M: velocity
n: density
0.2952
0.1505
1.0
0.5
0.0
−0.5
−1.0
2.0
1.5
1.0
0.5
0.0
0.2
0.4
0.6
0.8

Fig. 6(a)

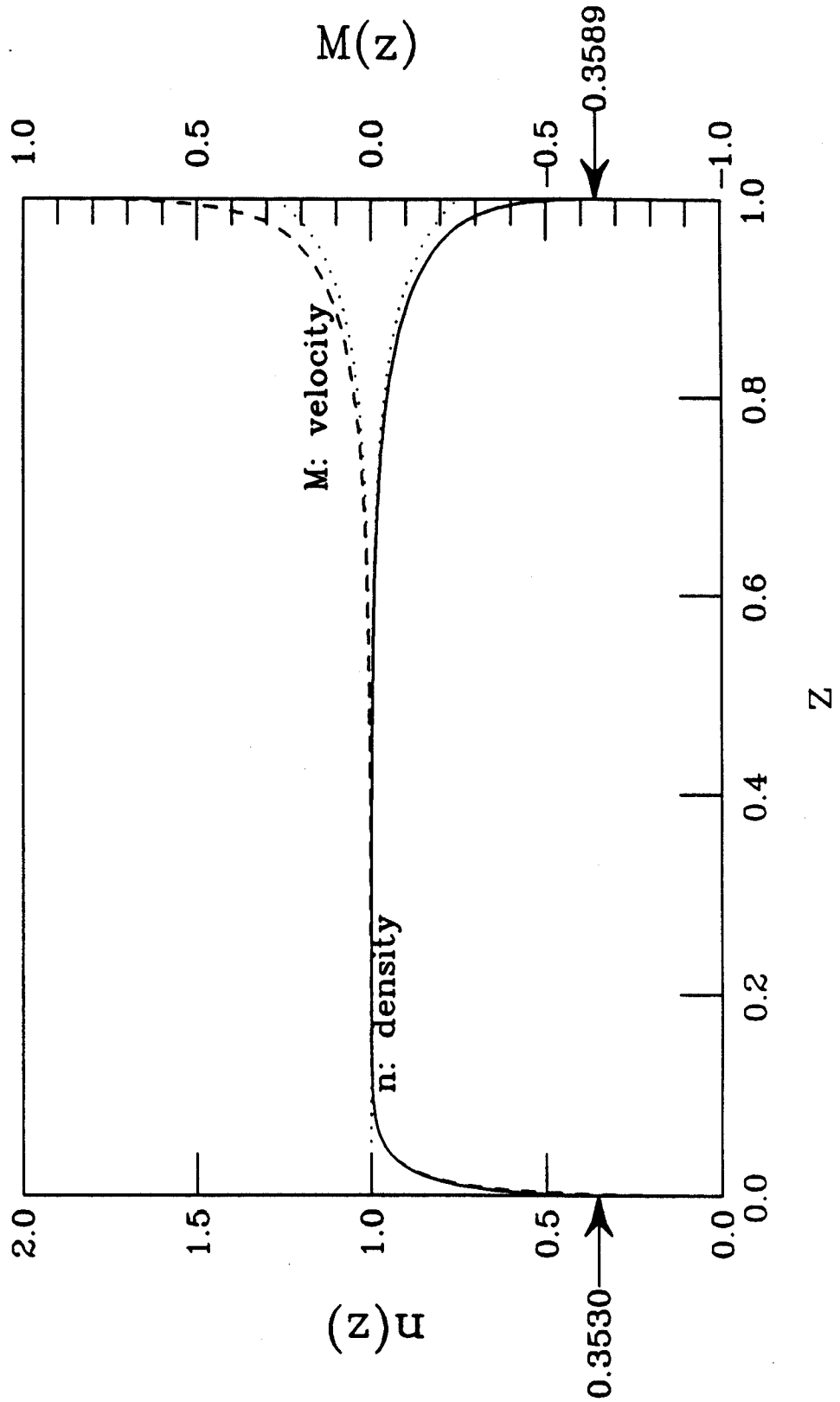
M(z)
1.0
0.5
0.0
−0.5
−1.0
0.3589
M: velocity
n: density
2.0
1.5
1.0
0.5
0.0
n(z)
0.3530
0.0
0.2
0.4
0.6
0.8
1.0
Z

Fig. 6(b)

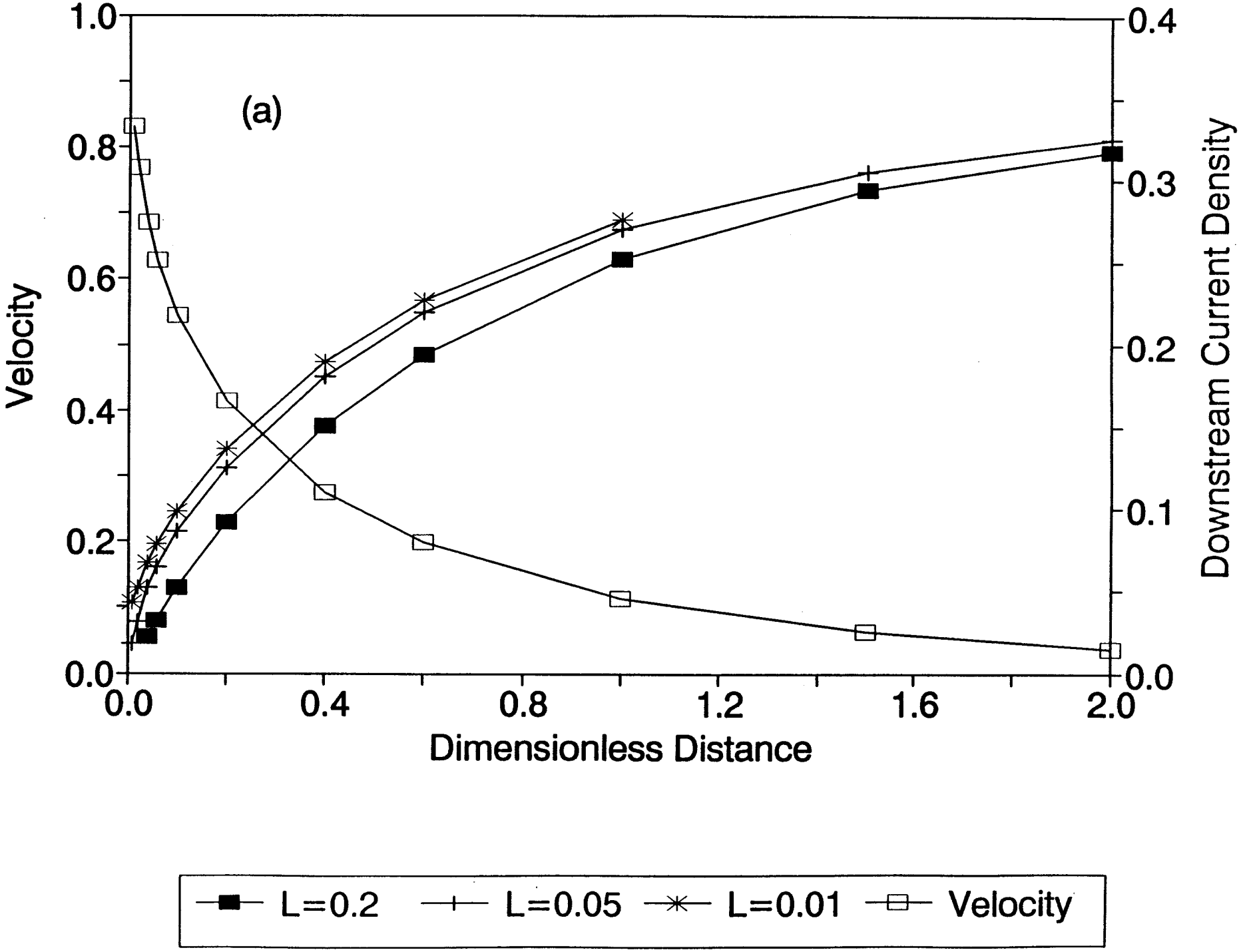
(a)
Velocity
Downstream Current Density
Dimensionless Distance
1.0
0.8
0.6
0.4
0.2
0.0
0.4
0.3
0.2
0.1
0.0
0.0
0.4
0.8
1.2
1.6
2.0
L=0.2
L=0.05
L=0.01
Velocity

Fig. 7(a)

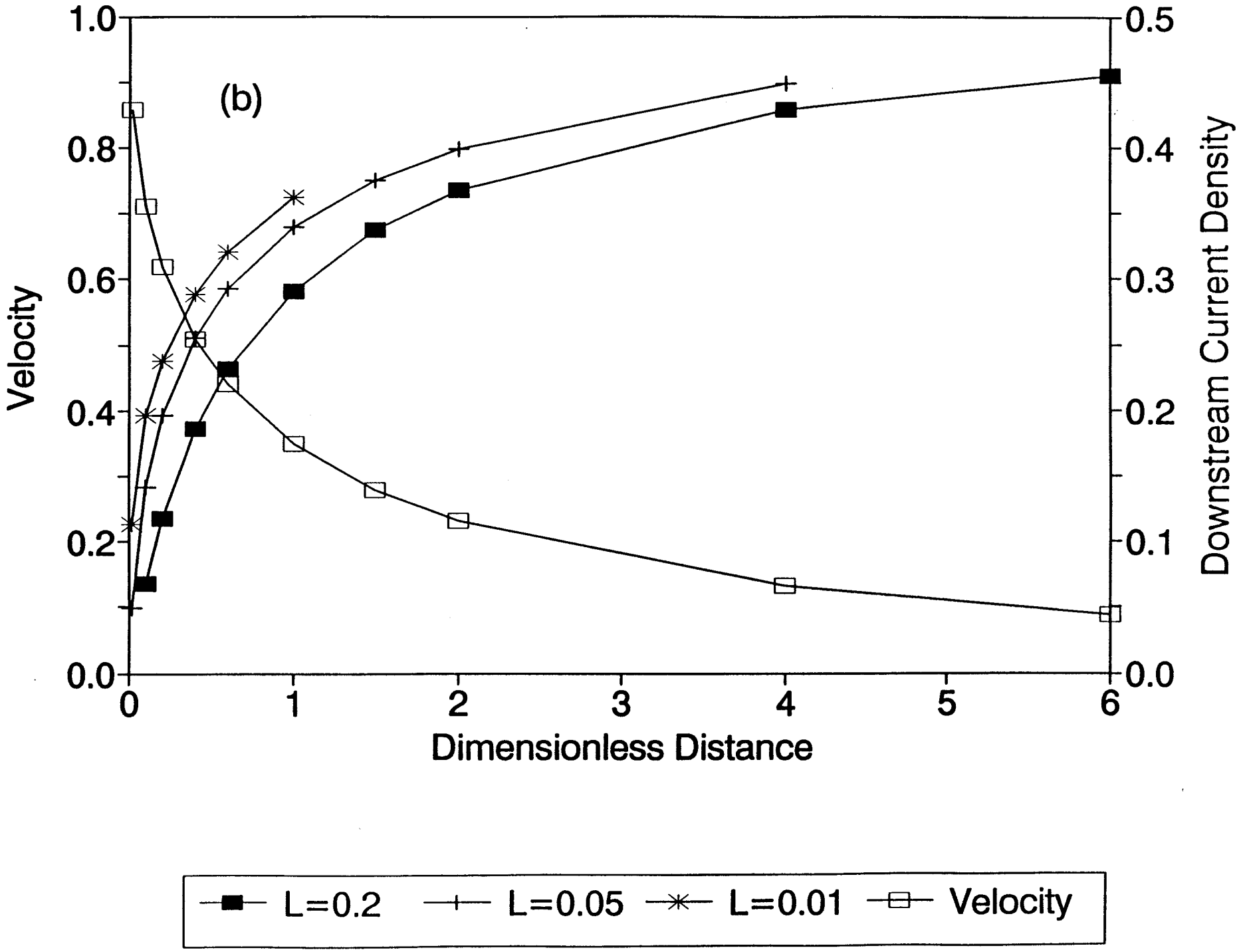
(b)
Velocity
Downstream Current Density
Dimensionless Distance
1.0
0.8
0.6
0.4
0.2
0.0
0.5
0.4
0.3
0.2
0.1
0.0
0
1
2
3
4
5
6
L=0.2
L=0.05
L=0.01
Velocity

Fig. 7(b)

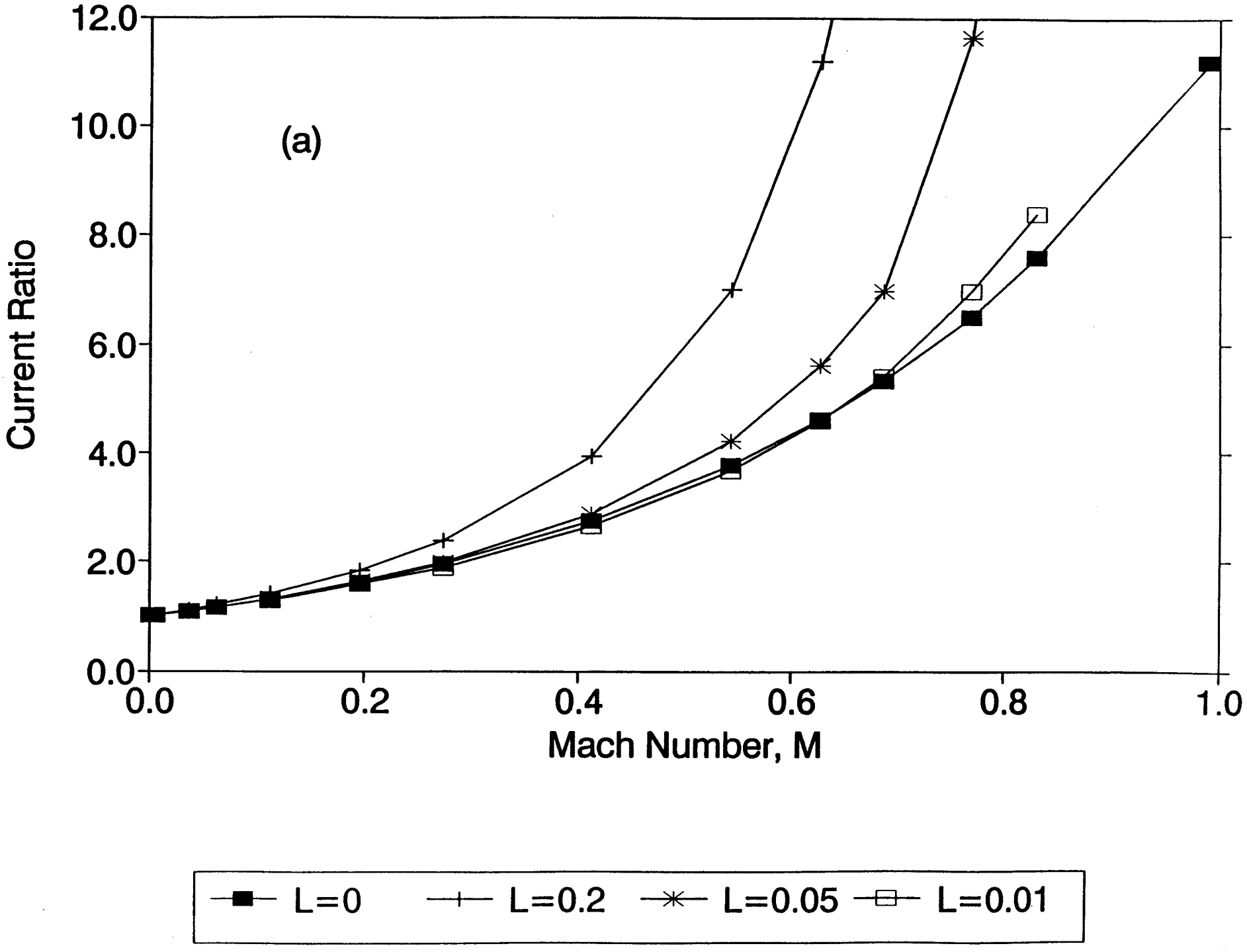
(a)
Current Ratio
12.0
10.0
8.0
6.0
4.0
2.0
0.0
0.0
0.2
0.4
0.6
0.8
1.0
Mach Number, M
L=0
L=0.2
L=0.05
L=0.01

Fig. 8(a)

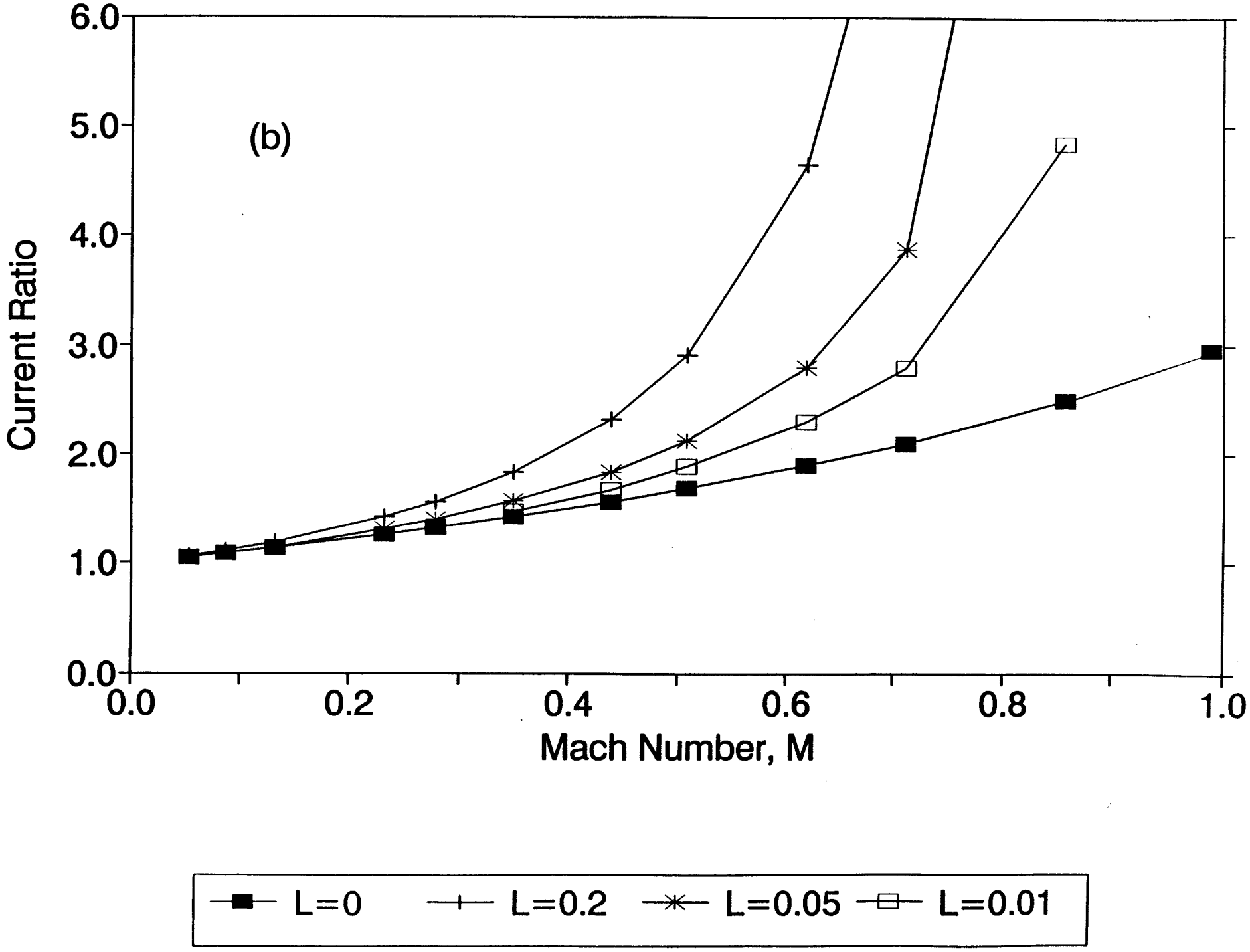
(b)
Current Ratio
Mach Number, M
6.0
5.0
4.0
3.0
2.0
1.0
0.0
0.0
0.2
0.4
0.6
0.8
1.0
L=0
L=0.2
L=0.05
L=0.01

Fig. 8(b)

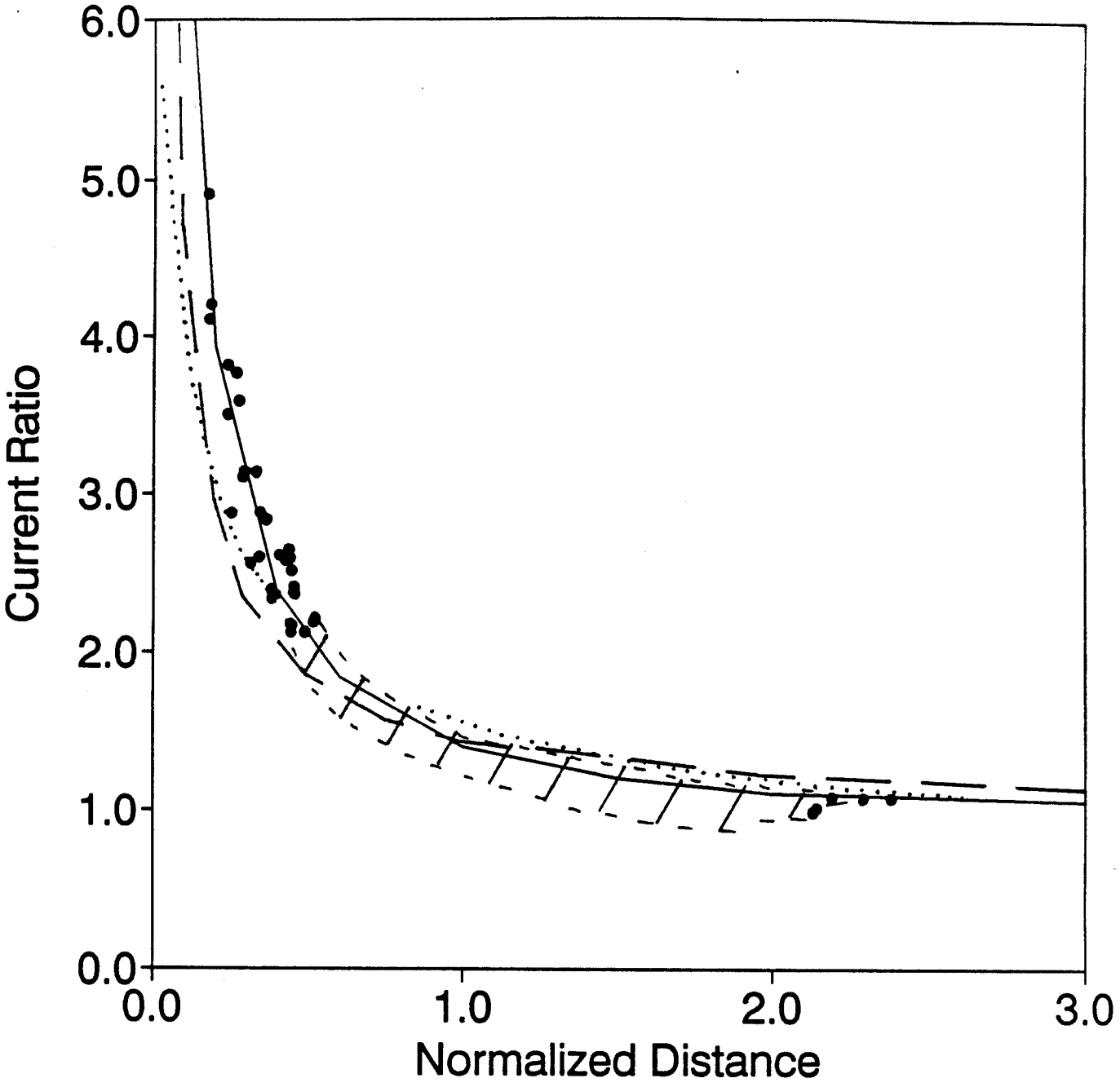
6.0
5.0
4.0
3.0
2.0
1.0
0.0
Current Ratio
0.0
1.0
2.0
3.0
Normalized Distance

Fig. 9